Journal of Thermal Analysis and Calorimetry, Vol. 55 (1999) 413-429

THE ACCURACY IN MICROWEIGHING IN VACUUM AND CONTROLLED ENVIRONMENTS

G. W. Chądzyński

Polish Academy of Sciences, W. Trzebiatowski Institute of Low-Temperature and Structure Research, 50-950 Wrocław 2, P. O. Box 937, Poland

Abstract

Accurate weighing depends on both physical factors and the weighing technique. There are two categories of physical factors: the location and support of the balance, and physical phenomena. Important such phenomena include processes of heat transfer by convection and radiation in rarefriction gases, Archimedes buoyancy, electrostatic, magnetostatic and gravitational effects, etc. Surveys of disturbances which affect the accuracy of weighing in vacuum or in controlled environments have been published elsewhere. This paper describes a high-vacuum apparatus connected to a Cahn RG ultramicrobalance. The system was adapted for investigations of long-time kinetic runs of oxygen loss in oxide superconductors in dynamic vacuum, and of other gas – solid interactions. Typical calibration curves for 'not fully compensated system' are presented in controlled environments at cryogenic temperatures.

Keywords: accuracy in microweighing in vacuum and controlled environments, vacuum microbalance techniques

Introduction

The majority of tests performed in a laboratory begin with the weighing of a sample. This emphasizes the importance of considering all possible sources of weighing errors.

Accurate weighing depends on both physical factors and the weighing technique. There are two categories of physical factors: the location and support of the balance, and physical phenomena. Important such phenomena include processes of heat transfer in rarefriction gases, Archimedes buoyancy, electrostatic and magnetostatic effects, etc.

The accuracy and reliability of weighing results not only depend on a precise measuring performance; they are also greatly dependent on the balance location. In order to set up an optimal weighing station, it is necessary to meet the following requirements: Whenever possible, the room in which the balance is located should be well thermostated temperature variation (about ±0.5 K). The corners

1418–2874/99/ $ 5.00

Akadémiai Kiadó, Budapest
Kluwer Academic Publishers, Dordrecht

of rooms are especially suitable as work locations because they are the most rigid locations in the building and are subject to the least amount of vibration.

To damp vibrations from the ground, rotating vacuum pumps, valves, etc., the balance must be fixed on a heavy stand. Under no circumstances should the balance be set up near a window. Otherwise, there is a risk that the balance can warm up unevenly because of exposure to direct sunlight. If heat or cold is produced by ovens or liquefied gases, protective shields should be placed above these devices.

For lighting needs, the best solution is artificial light in a room without windows. Light fixtures must be sufficiently far from the weighing stand. To prevent disturbing thermal radiation, high-wattage lamps should not be installed. It is recommended the fluorescent lighting be used.

The most important disturbances which affect the accuracy of weighing in vacuum or in a controlled atmosphere are as follows [1–3]:

- Brownian motion
- Knudsen forces
- Convective currents in the balance chamber
- Archimedes buoyancy
- Cavity force
- Unequal thermal expansion of the balance arms
- Radiation pressure
- Magnetostatic effects
- Electrostatic effects
- Vibrations of the building
- Sorption effects and contamination
- Other effects

Numerical estimates of the disturbing phenomena for beam-type balances have been published by others [4]. Weighing in the pressure region where the Knudsen forces exhibit their maximum (about 1 Pa) must be avoided. Czanderna [5] developed methods to correct mass in the region of TMF (thermomolecular flow). After the pressure effect has been determined for an inert gas (e.g. nitrogen), the reacting gas (oxygen) is admitted in similar pressure increments.

The mass gained by the sample is the difference in mass readings between the two curves.

Another method consists in diluting the reacting gas with an inert gas. This technique depends on maintaining the total pressure in the system at pressures higher than the region of TMF.

Experimental

The high-vacuum apparatus connected to the Cahn RG ultramicrobalance is illustrated schematically in Fig. 1. The system previously described for measure-

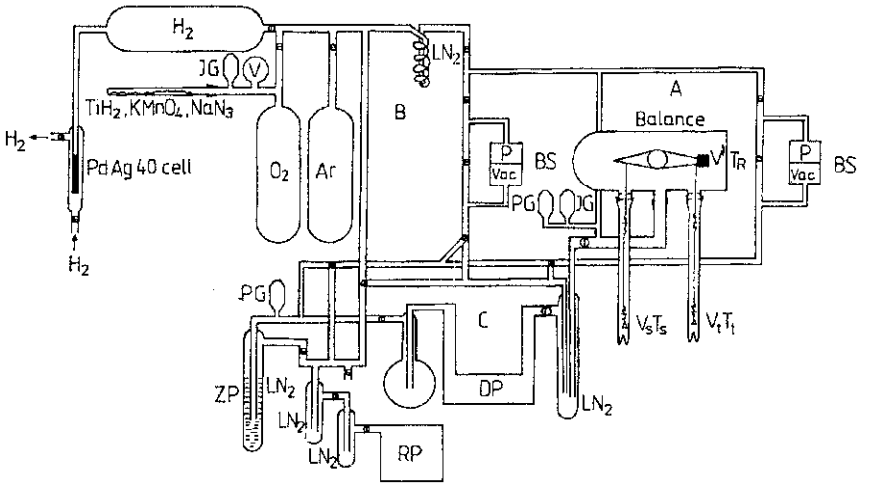

Fig. 1 Experimental apparatus: Balance, DP – diffusion pump, RP – rotary pump, LN_2 – liquid nitrogen trap, PG – Pirani gauge, IG – ionization gauge, V – vacuummeter, BS – Barocel sensor

ments of gas sorption on metallic catalysts [6] was adapted for investigations of long-time kinetic runs of oxygen loss in oxide superconductors in dynamic vacuum [7, 8], and of other gas – solid interactions.

The experimental apparatus consists of three connected independent loops, A, B and C. A: the Cahn ultramicrobalance assembly with the measuring system, B: the gas handling and purification system, and C: the pumping system.

The balance chamber and an all-glass manifold can be evacuated to 10^{-7} torr through an air-cooled oil diffusion pump. A large liquid-nitrogen trap (500 mm in length), located directly above the diffusion pump, isolates the pump from the other parts of the apparatus and serves to prevent contamination by diffusion pump oil. A zeolite pump is installed between the oil diffusion pump and the rotary forepump to allow for continuous pumping for several weeks.

When evacuated, the pressure in the manifold is determined by the Pirani and ionization gauges. A capacitance manometer (Datametrics, model 1083 with two Barocel sensors, 523–15 and 523–12) is used to measure pressures from 10^{-3} to 10^{3} torr.

The gas handling system is used to introduce and remove gases from the balance chamber. The principal part of this system is an all-glass manifold which can be evacuated through the pumping system. Hydrogen was purfied by passing it through a heated palladium diffusion cell and next stored as titanium hydride, TiH_2. Oxygen and nitrogen were generated by thermal decomposition of $KMnO_4$ and NaN_3 (Fluka p.a.), respectively. A rough estimation of the pressure in the gas inlet part of the system was possible with a Bourdon vacuummeter.

The balance is installed in Pyrex glass chamber supplied by the manufacturer. To reduce the transfer of building vibrations, the balance chamber is mounted on

a separate steel support bolted to a frame on the room wall. The frame also serves to suppress vibrations from the room that might affect the performance of the balance.

The sample is placed in a fused silica pan 10 mm in diameter and suspended via a hangdown fused silica wire 0.3 mm in diameter connected to loop A of the balance beam and enclosed within a hangdown tube 550 mm in length.

To minimize the Knudsen and Archimedes forces, an identical hangdown tube and symmetrical suspension are used on the tare side of the balance. To prevent disturbances by thermal gas flow, disk screens made of fused silica, 10 mm in diameter, are installed above the pan to reduce heat radiation from the room and to protect the sample against recontamination. When turned upside down, the screens are used to hold calibration masses during the preliminary calibration of the balance electronics.

The total mass of the suspension is ca 300 mg. Additionally, steel collars are mounted in the inner joints of the balance chamber. An 8 mm opening in the middle of each ring facilitates proper positioning of the balance within the chamber and centring of the pans within the hangdown tubes.

The temperature of the sample and tare is maintained by temperature-programmed, well-insulated, non-inductively wound furnace 150 mm in length, placed around each hangdown tube.

The temperature in the vicinity of the sample is measured by a NiCr–Ni thermocouple (Heraeus) with a nominal accuracy of 0.2 K, located within 2 mm of the sample pan. This may be very close to the furnace wall [9]. The output from the thermocouple is displayed on a digital microvoltmeter.

The balance beam (ν', T_R) of the Cahn balance has been found to exhibit a small reproducible, pressure-dependent apparent mass change, which can not be eliminated because of the design of the balance.

The experimental arrangement used minimizes, but does not eliminate TMF. The remaining forces have been found to be reproducible for a fixed geometry and have been determined from blank runs on the system. For blank runs, the hangdown tubes are submerged to a depth of 100 mm in liquid nitrogen or in liquid oxygen contained in two open dewars.

The temperatures of the cryogenics baths are measured by means of a suitable gas thermometer. The real temperatures of the cryogenics baths are a little higher. The deviations of T from the nominal values did not exceed 2 K.

All sources of thermal radiation are carefully shielded by using thermal insulation. A box made of perforated steel provides thermal, mechanical, electrostatic and light shielding of the balance chamber.

Results and discussion

Figure 2 depicts a plot of apparent mass change *m vs.* pressure for the beam and symmetrical suspension in controlled environments at cryogenic temperatures.

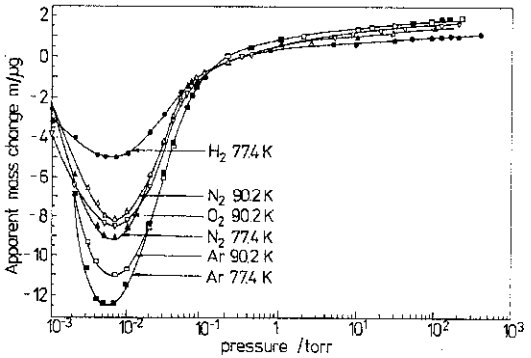

Fig. 2 Plot of apparent mass change m (μg) *vs.* pressure for the beam and symmetrical suspension in controlled environments at cryogenic temperatures

All the calibration curves exhibit a negative apparent mass change below 0.3 torr, with a minimum at 10^{-2} torr and an apparent increase in the mass at higher pressures, which appears to be a linear function of pressure above 50 torr.

The plot has a minimum at 10^{-2} torr, varying from –13 μg for argon to – 9 – –8 μg for nitrogen and oxygen, and –5 μg for hydrogen.

This behaviour is found to be highly reproducible and is thought to be associated with the light source in the null detection system of the Cahn balance. Since the light source is necessary for the operation of the balance, the effect cannot be eliminated, but must be taken into account in the calibration of the system.

The results of numerical estimation of disturbing effects [4] and many experimental papers [1] indicate that the most important sources of measuring errors in studies of gas – solid interactions include mainly:

– buoyancy errors, proportional to the increase in pressure

– fictitious changes in mass, caused by Knudsen forces, due to thermal gas motion at pressure below 10 torr (10^3 Pa) [1–3].

The course of the curves at low pressures is characteristic of thermal flow gases: TMF and slip flow as a result of radiometric forces [1–3, 10, 11]. The linear portion of the curves at higher pressures is due to buoyancy force [1–3]. A buoyancy force F will exist if an unequal volume, Δv, is occupied by the beam, suspension, sample and tare pans, etc. For a gas obeying the equation of state, $pv=nRT$, the mass of the gas displaced is given by

$$F/g = m = PM\Delta v/RT \quad (1)$$

where P is the pressure in torr, M is the molecular mass of the gas, Δv is the displaced volume, n is the number of moles, T is the absolute temperature, and R is the universal gas constant.

The buoyancy effect on the mass is a function with four variables. The advantage of a symmetric system is now evident, since Δv is the only parameter that

can be designed to be zero. Aranging Δv to be zero initially is a necessary, but not complete solution; the sample, counterweight, and heated or cooled parts of the suspensions must also have the same volume, to eliminate the temperature dependence of Δv.

When real gases are employed, care must be taken to use the equation of state that is appropriate for the gas, temperature and pressure conditions of the experiment. For a more accurate calculation of this correction, it is necessary to take into account Coulomb forces and inhomogeneities in the surface structure of the sample (micropores if the surface area of the sample is greater than 1–100 m^2/g), which generally increase the binding forces and hence lead to a greater positive correction [3, 5].

If the sample temperature deviates from the temperature of the balance, thermal gas flow is produced, exerting forces and resulting in spurious mass changes. The critical pressure is characterized by the Knudsen number $K_n=1$, where $K_n=\lambda/d$ is defined as the ratio of the mean free path λ of a gas molecule before it strikes another molecule, and d is a characteristic length of the apparatus, e.g. the tube or vessel diameter.

At $K_n \geq 1$, TMF may be expected. The gas molecules exchange momentum almost exclusively with the walls of the pans or equipment, rather than with one another.

Temperature differences along the tube result in a pressure difference, the maximum of which is defined by the Knudsen formula $p_1/p_2=\sqrt{T_1T_2}$ where p is the pressure and T is the absolute temperature.

For pressures where $K_n=0.1$, the mean free path λ can be calculated from a relation developed from kinetic theory:

$$\lambda \leq kT/\sqrt{2\pi pL^2} \tag{2}$$

where k is the Boltzmann constant, T is the absolute temperature, p is the pressure and L is the diameter of the molecule. In this range, slip flow occurs along a surface in which temperature differences exist, the layer thickness corresponding approximately to the mean free path.

The reaction force is directed from warm to cold. TMF and slip flow result from the difference between the mean velocities of the gas molecules coming from hot to cold zones. They also depend on the gas pressure, which alters the mean free path of the gas molecules [3]. These two types of flow give rise to Knudsen forces on the balance and produce an apparent mass change at low pressures. The occurrence of transversal or longitudinal effects depends on the geometry, and on whether the force acts on a surface normal to or parallel to the temperature gradient [2, 3].

The actual shape of these curves appears to be the result of the nature and pressure of the gas present.

Similar, but not identical curves have been obtained elsewhere [1].

The contribution of the balance beam accounts for a mass correction, presumably as a result of asymmetrical heating of the beam in the region flag and small asymmetry of the beam [ν', T_R] in Fig. 1.

Gravimetric methods are very useful in experimental adsorption studies. The possibility of independent recording of the adsorbant mass and adsorbate pressure in every step of the experiment is their main advantage over the volumetric methods. The application of a gravimetric technique for measurement of the adsorption isotherms for argon, nitrogen, oxygen and hydrogen at 77.4 K and 90.2 K on γ-alumina are presented. γ-Alumina is a typical support of catalysts and the low-temperature adsorption of simple gases may be used for the evaluation of its surface area.

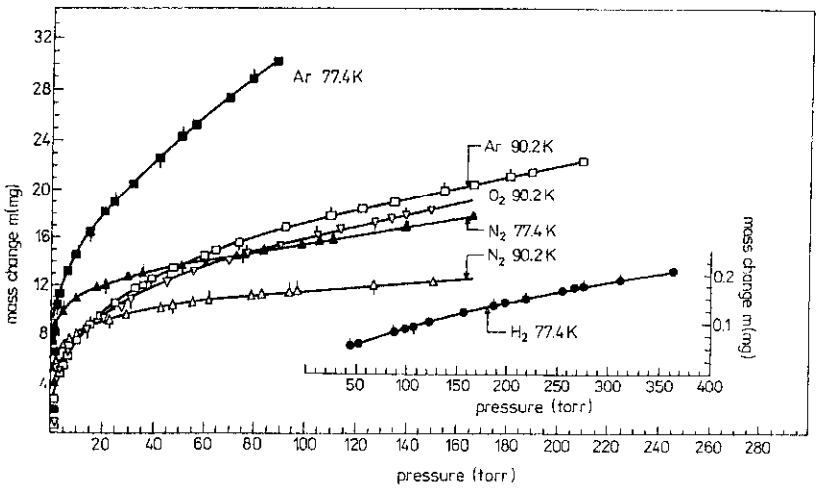

Fig. 3 Mass changes during adsorption of argon, nitrogen, oxygen and hydrogen on a sample of γ-Al_2O_3 outgassed at 673 K (m=180.6 mg). The upper and lower marks denote desorption and reversible adsorption, respectively. (After Kubicka and Chądzyński [12])

Figure 3 presents the corrected mass changes m of a sample outgassed at 673 K as a function of the adsorbate pressure p. The increases in mass of the sample resulting from the adsorption of argon, nitrogen, oxygen and hydrogen were 0.35–30.20, 1.59–17.67, 0.78–18.18 and 0.052–0.202 mg, respectively. All the adsorption isotherms were reversible in the sense that increasing and decreasing pressures gave the same isotherms, and that the adsorbates could be completely removed by pumping at the temperature of the experiment.

The isotherms were analysed by means of the BET equation. The corresponding plots are shown ing Fig. 4. They illustrate the applicability of the BET equation to the adsorption of argon, nitrogen and oxygen in the conventional range of relative pressures $0.03<p/p_c<0.30$ (p_c is the vapour pressure of the adsorbate in the liquid state). The adsorption of hydrogen at 77.4 K covering the range of rela-

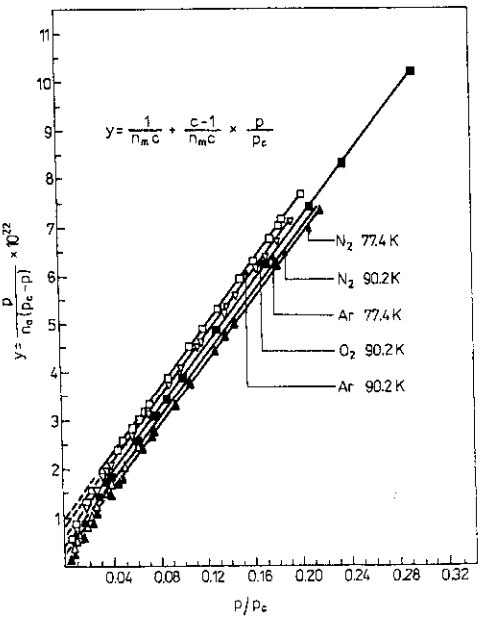

Fig. 4 BET isotherms for argon, nitrogen and oxygen

tive pressures below 0.003 is described elsewhere [12] by the DR (Dubinin-Radushkevich) equation.

Table 1 lists the parameters of the BET straight lines determined by the method of least squares. The monolayer quantities n_m found for argon, nitrogen and oxygen by using the BET plots are consistent within experimental error.

The average surface area a_s of γ-alumina, as determined from argon adsorption by using the BET parameter n_m and molecular area a_m derived from the liquid density, is 230 $m^2 g^{-1}$ or 41.5 m^2 per sample. The similar determination for oxygen adsorption gave nearly the same result, while the surface area determined from nitrogen adsorption was several per cent higher. The heats of adsorption q_a for argon, nitrogen and oxygen adsorption, calculated from the BET constants c and referring to a surface coverage Θ close to unity, are 2.1–2.3 kcal mol^{-1} and exceed the heats of liquefaction q_c by about 0.7 kcal mol^{-1} [12].

As already reported [13], the adsorption capacity of the investigated γ-alumina decreased considerably when its outgassing temperature was increased from 673 to 773 or to 823 K. The average values of n_m determined from argon adsorption by using the BET equation fell to 11.7×10^{20} and 11.4×10^{20} molecules g^{-1}, respectively. The surface area of the sample was about 165 $m^2 g^{-1}$. The gravimetric dehydration and X-ray data indicated that the effect was connected with sintering and not with a phase transition of the oxide.

The study of hydrogen and oxygen chemisorption and of hydrogen – oxygen titration in a wide temperature range on supported metallic catalysts is very use-

Table 1 Parameters of the BET isotherms

Adsorbate	T_a/ K	$n_m \times 10^{-20}$/ mol	$n_m \times 10^{-20}$/ mol g^{-1}	Θ^*	a_m^{**}/ Å^2	c	a_s/ $m^2 g^{-1}$	q_a/ kcal mol^{-1}***
Argon	77.4	2.99	16.6	0.73–1.38	13.8	229	64	2.2
	90.2	2.91	16.1	0.63–1.20	14.4	232	39	2.2
Nitrogen	77.4	2.98	16.5	0.94–1.31	16.2	267	148	2.1
	90.2	2.79	15.2	0.82–0.89	17.1	260	155	2.2
Oxygen	90.2	3.01	16.7	0.64–1.14	14.1	235	41	2.3

*Experimental range of the coverages, at wich the BET equation was applicable.
**Molecular area calculated from the liquid density.
***1 kcal=4.19 kJ.

ful for characterization of the catalysts. It affords information concerning the chemisorption features and other important properties of the catalysts, such as the parameters of reduction and oxidation or the surface area and dispersion of the supported metal. The graivmetric method allows determination of the kinetics and reversibility of sorption, and direct control of the processes of reduction, oxidation or outgassing of the catalysts.

A study of hydrogen and oxygen sorption on γ-alumina-supported rhenium seemed of considerable interest as it is widely used as a catalyst or catalyst promoter [14, 15].

Investigations of hydrogen and oxygen sorption and of hydrogen – oxygen titration on Re/γ-alumina catalyst containing 10.4 wt% of the metal have been made with respect to time, pressure and temperature. The pressures and temperatures applied for hydrogen sorption varied in the ranges 50–250 torr and 293–823 K.

Gradually increasing temperatures were applied and at each temperature the total and reversible sorption were measured at increasing pressures. The total sorption of hydrogen was measured in two ways: (A) on the sample cooled *in vacuo* from 823 K to the temperature of measurement; and (B) by saturating the sample with hydrogen from 823 K to the temperature of measurement.

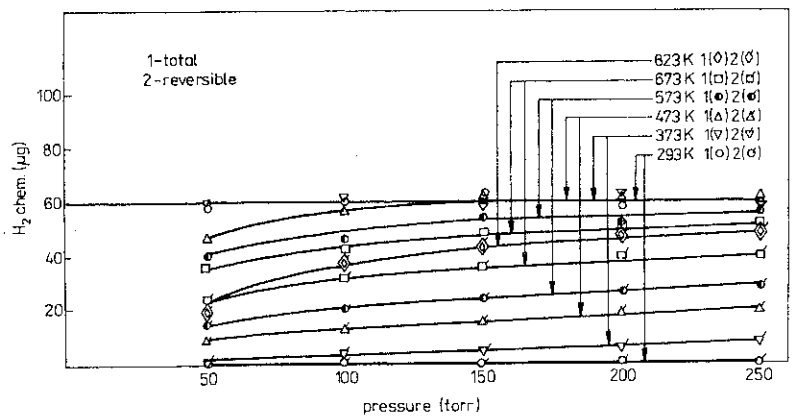

Fig. 5 Chemisorption of hydrogen using procedure B *vs.* pressure on a sample of the 10.4 wt% Re/γ-Al_2O_3 catalyst (m=304.1 mg). (After Chądzyński and Kubicka [6])

Figures 5 and 6 present the chemisorption data on supported rhenium, determined by taking into account the calibration corrections for the γ-alumina support. Figure 5 shows the total and reversible chemisorption as a function of pressure at all the applied temperatures, obtained according to procedure B on a sample of 10.4 wt% Re/γ-Al_2O_3 catalyst. Figure 6 depicts the chemisorption determined on the 10.4 wt% Re/γ-Al_2O_3 catalyst at 250 torr as a function of temperature, the amount of chemisorbed hydrogen being given in molecules per g of the catalyst (molecules (g cat)$^{-1}$). It can be seen from Figs 5 and 6 that the chemi-

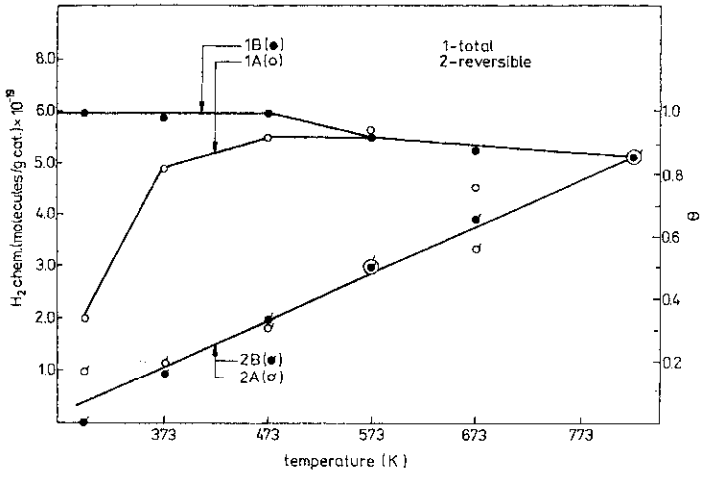

Fig. 6 Chemisorption of hydrogen *vs.* temperature at 250 torr on the 10.4 wt% Re/γ-Al_2O_3 catalyst

sorption of hydrogen on the catalyst is activated in nature. On the sample of the catalyst cooled *in vacuo* to the temperature of measurement (procedure A), the extent of chemisorption increased with increasing temperature and reached its maximum value at 573 K (Fig. 6). The results obtained below 573 K were much higher when the catalyst was saturated with hydrogen from 823 K (procedure B). In this case, the total amount of chemisorbed hydrogen reaches its maximum value at 293–473 K. At these temperatures, the chemisorbed amounts obtained according to procedure B are independent of pressure over the whole range, or above 100 torr, indicating saturation. The maximum total amount of hydrogen chemisorbed on the catalyst at saturation at 293–473 K, according to procedure B, is 60 μg for the sample with a mass of 304.1 mg, or 5.94×10^{19} molecules $(g\ cat)^{-1}$. Thus, a larger portion of the hydrogen chemisorption at room temperature at saturation is due to slow activated chemisorption.

From the data given in Figs 5 and 6, it also follows that at each temperature below 823 K, both irreversible and weaker reversible chemisorption occurs. At room temperature, the reversible chemisorption does not exceed 10% of the maximum value. At 573 K, it constitutes 40–60% of the total chemisorption typical of that temperature: about 30% of the maximum value. At 823 K, the chemisorption is totally reversible and constitutes 80% of the maximum value. These results indicate the energetic heterogeneity of the rhenium surface under study. The maximum total amount of hydrogen chemisorbed on the catalyst at room temperature according to procedure B was used to calculate the coverage of the rhenium surface with hydrogen, Θ, and also to calculate the quantities characterizing the dispersion of the supported rhenium [6].

The earlier-reported results of the measurement of oxygen sorption by the catalyst [16] are presented in Fig. 7 and in Table 2. Figure 7 shows the change in

oxygen sorption with time on the catalyst sample in the form of Elovich plots: mass change m *vs.* log$t$ [17–19]. Table 2 lists the amount of sorbed oxygen, $O_{2\text{-chem}}$, per mg sample and in molecules per g of catalyst (molecules $(g\ cat)^{-1}$) as functions of time and temperature. The corresponding values of the ratios O/H and O/Re are also given in Table 2. These are the ratios of the number of sorbed oxygen atoms to the number of hydrogen atoms chemisorbed in the monolayer and to the total number of rhenium atoms in the catalyst.

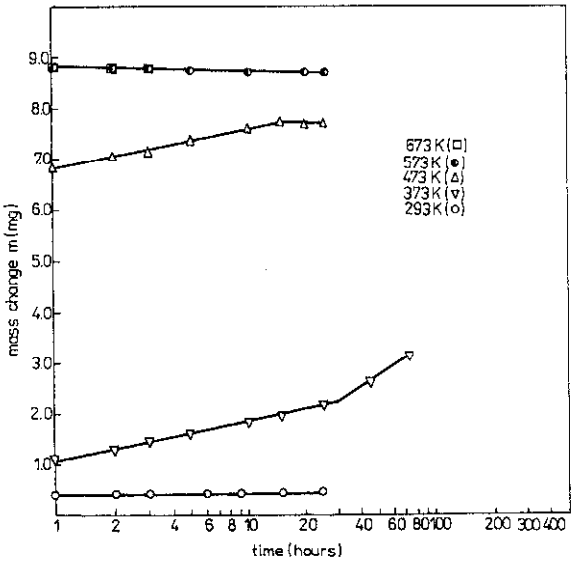

Fig. 7 Elovich plots for sorption of oxygen at 100 torr on a sample of 10.4 wt% Re/γ-Al_2O_3 catalyst (m=306.6 mg). (After Chądzyński and Kubicka [16])

All the results given in Table 2 were found to be completely irreversible, independently of pressure. The results demonstrate above all that the sorption of oxygen by the catalyst is a slowly activated process.

For the catalyst below 673 K, a portion of the oxygen was sorbed rapidly over 1 min; following that sorption, however, a much slower mass change was recorded. At 293 and 373 K, saturation of the catalyst sample with oxygen was not attained after contact of the sample with oxygen for 25 or 72 h, respectively. At 473 K, the mass increase in oxygen was established only after several hours, whereas at 573 K, this was done within 30 min, and at 673 K, after 1 min.

The irreversibility, and also the presence of a slowly activated component of the sorption, suggest that the interaction of oxygen with the catalyst involves not only chemisorption on the surface of the rhenium, but also oxidation of the bulk rhenium. This is confirmed by the values of the ratios O/H and O/Re given in Table 2.

With elevation of the temperature, the ratio O/H increases. At 573 and 673 K, it attains the high value of 9.10, indicating considerable oxidation of the bulk

Table 2 Sorption of oxygen on the 10.4 wt% $Re/\gamma\text{-}Al_2O_3$ catalyst

T/ K	t/ h	$O_{2\text{-chem}}$/ mg	$O_{2\text{-chem}}$/ mol (g cat)$^{-1}\times10^{-20}$	O/H	O/Re
293	1/60	0.25	0.15	0.26	0.09
	1/4	0.30	0.18	0.31	0.11
	1/2	0.35	0.22	0.36	0.13
	1	0.40	0.24	0.41	0.15
	3	0.42	0.26	0.43	0.15
	6	0.50	0.31	0.52	0.18
	9	0.51	0.31	0.53	0.19
	25	0.55	0.34	0.56	0.20
373	1/60	0.80	0.49	0.83	0.30
	1/4	1.05	0.64	1.08	0.38
	1/2	1.10	0.68	1.14	0.40
	1	1.20	0.74	1.24	0.44
	2	1.30	0.80	1.34	0.47
	5	1.55	0.95	1.60	0.57
	10	1.90	1.17	1.96	0.70
	15	2.05	1.26	2.12	0.75
	20	2.20	1.35	2.27	0.80
	25	2.30	1.41	2.38	0.84
	45	2.74	1.68	2.83	1.00
	72	3.34	2.05	3.45	1.22
473	1/60	4.40	2.70	4.55	1.61
	1/4	6.00	3.68	6.20	2.20
	1/2	6.55	4.02	6.77	2.40
	1	6.80	4.18	7.03	2.48
	3	7.20	4.42	7.44	2.63
	5	7.40	4.54	7.64	2.70
	10	7.70	4.72	7.96	2.81
	15	7.80	4.79	8.06	2.85
	20	7.80	4.79	8.06	2.85
	25	7.80	4.79	8.06	2.85

Table 2 Continued

T/ K	t/ h	$O_{2\text{-chem}}$ mg	$O_{2\text{-chem}}$ mol (g cat)$^{-1}\times10^{-20}$	O/H	O/Re
573	1/60	8.40	5.16	8.68	3.07
	1/4	8.55	5.25	8.83	3.12
	1/2	8.80	5.40	9.10	3.22
	1	8.80	5.40	9.10	3.22
	–	–	–	–	–
	–	–	–	–	–
	–	–	–	–	–
	25	8.80	5.40	9.10	3.22
673*	1/60	8.80	5.40	9.10	3.22
	1/4	8.80	5.40	9.10	3.22
	1/2	8.80	5.40	9.10	3.22
	1	8.80	5.40	9.10	3.22
	2	8.80	5.40	9.10	3.22
	3	8.80	5.40	9.10	3.22

* Because of the observed Re_2O_7 volatilisation, measurements were made for 3 h only

rhenium. At these temperatures, the ratio O/Re reaches 3.22, which is only 8% lower than the value of 3.5 corresponding to complete oxidation of rhenium to rhenium heptoxide, Re_2O_7. The ratio may be underestimated because of the possibility of volatilization of the rhenium heptoxide formed [20]. Indeed, this was indicated by the appearance of a grey deposit on the inner wall of the hangdown tube above the sample container.

The hydrogen – oxygen titrations indicate that the reaction of hydrogen with chemisorbed oxygen is possible only at elevated temperatures. It is accompanied by an increase in the mass of the catalyst at slightly elevated temperatures, and by a decrease in the catalyst mass at sufficiently high temperatures. During rapid heating in hydrogen up to 823 K, the sample of the catalyst oxidized at 293 K initially increased in mass. The mass increase attained a maximum at 438 K for the 10.4 wt% Re/γ-Al_2O_3 catalyst. Above that temperature, the mass of the sample decreased.

Table 3 lists the results of titrations performed under isothermal conditions over the temperature range 293–438 K for the 10.4 wt% Re/γ-Al_2O_3 catalyst. For the catalyst sample oxidized at 293 K over 3, 6, 9 or 25 h, the maximum increase in hydrogen content observed at 438 K is consistent with the calculated amount of hydrogen necessary to react with the chemisorbed oxygen and for chemisorp-

Table 3 Hydrogen – oxygen titration on a sample of the 10.4 wt% Re/γ-Al_2O_3 catalyst (m=306.6 mg)

T_{chem}/ K	t_{chem}/ h	$O_{2\text{-chem}}$/		T_{titr}/ K	$H_{2\text{-titr, exp}}$/		$H_{2\text{-titr, calc}}$/ mol (g cat)$^{-1}\times10^{-19}$
		mg	mol (g cat)$^{-1}\times10^{-19}$		mg	mol (g cat)$^{-1}\times10^{-19}$	
293	3	0.42	2.58	293	0.000	0.00	7.00
		0.42	2.58	373	0.055	5.40	8.40
		0.42	2.58	438	0.090	8.90	8.70
293	6	0.50	3.07	293	0.000	0.00	8.00
		0.50	3.07	373	0.055	5.40	9.40
		0.50	3.07	438	0.100	9.80	9.60
293	9	0.51	3.13	293	0.000	0.00	8.10
		0.51	3.13	373	0.055	5.40	9.50
		0.51	3.13	438	0.100	9.80	9.80
293	25	0.55	3.38	293	0.000	0.00	8.60
		0.55	3.38	373	0.055	5.40	10.00
		0.55	3.38	438	0.110	10.80	10.30
373	25	2.30	14.1	373	0.140	13.70	31.50
		2.30	14.1	438	0.160	15.70	31.70
373	45	2.74	16.8	373	0.140	13.70	36.90
		2.74	16.8	438	0.180	17.70	37.10

T_{chem} and t_{chem}, Temperature and time of oxygen chemisorption; $O_{2\text{-chem}}$, amount of chemisorbed oxygen; T_{titr}, temperature of hydrogen – oxygen titration; $H_{2\text{-titr, exp}}$, experimental amount of hydrogen taken up during titration for 3 h; and $H_{2\text{-titr, calc}}$, $O_{2\text{-chem}}\times2H_{2\text{-chem}}$, total calulated amount of hydrogen required during titration.

tion on the bare rhenium surface. At 373 K, the experimental titration result is 40% lower than the calculated value. At 293 K, the titration result is zero, i.e. no change in hydrogen mass was observed for the catalyst sample oxidized at the same temperature. The titration result at 438 K for the sample oxidized at 373 K for 25 or 45 h is much lower than the calculated value. It may be concluded that, in the case of the catalyst at 438 K, all the oxygen chemisorbed at 293 K reacts with hydrogen. The water resulting from the reaction is desorbed from the surface of the rhenium and the chemisorption of hydrogen typical for a bare surface of rhenium then takes place. The water is trapped by the support, but is not desorbed over the 3 h period of the experiment. Oxygen sorbed at 373 K reacts only partially with hydrogen at 438 K. At 373 K, it is not possible for oxygen sorbed at 293 or 373 K to react completely with hydrogen. At 293 K, hydrogen does not react or reacts only very slowly with sorbed oxygen. At that temperature, the chemisorption of hydrogen on the rhenium surface covered with oxygen in amounts corresponding to 43–56% of the monoatomic layer does not occur or is exceedingly slow.

The decrease in mass of the oxidized sample of the catalyst in hydrogen above 438 K must be due to reduction of the catalyst and removal of oxygen from it in the form of water generated during the reduction by hydrogen of the supported rhenium oxide.

The complete reduction of the oxides should be matched by a decrease in the mass of the catalyst to its initial value, recorded after reduction and outgassing at 823 K and prior to the sorption of oxygen.

It follows from the results that the reaction of hydrogen with oxygen chemisorbed on the surface or bound in the body of the rhenium occurs only at appropriately elevated temperatures. At only slightly elevated temperatures, the reaction is confined to oxygen chemisorbed on the rhenium surface. Reduction of the volume of rhenium oxides is conditioned by the desorption of the water formed as a product of the reduction not only from the rhenium, but also from the support, and is possible only at sufficiently high temperatures.

Application of the gravimetric method to hydrogen – oxygen titration at 293–823 K permits a distinction between the reactions of hydrogen with chemisorbed oxygen occurring on the surface and in the body of the rhenium. The reactions are slow or very slow and occur only at suitably high temperatures.

Conclusions

The experimental arrangement used minimized but did not eliminate TMF. The remaining forces were found to be reproducible for a fixed geometry and were determined from blank runs on the system.

The contribution of the balance beam accounts for mass correction is a result of asymmetrical heating of the beam in the region flag and small asymmetry of the beam, because the influence of the design of the balance can not be eliminated.

References

1 A. W. Czanderna and S. P. Wolsky, in A. W. Czanderna and S. P. Wolsky (Eds.) 'Microweighing in Vacuum and Controlled Environments', Elsevier, Amsterdam 1980, p. 1.
2 C. H. Massen and J. A. Poulis, ibid., p. 95.
3 R. Sh. Mikhail and E. Robens, 'Microstructure and Thermal Analysis of Solid Surfaces', Wiley Heyden Ltd., Chichester 1983.
4 C. H. Massen, E. Robens, J. A. Poulis and Th. Gast, Thermochim. Acta, 82 (1984) 43, 103 (1986) 39.
5 A. W. Czanderna, in A. W. Czanderna and S. P. Wolsky (Eds.) 'Microweighing in Vacuum and Controlled Environments', Elsevier, Amsterdam 1980, p. 175.
6 G. W. Chądzyński and H. Kubicka, Thermochim. Acta, 158 (1990) 353.
7 G. W. Chądzyński J. Stępień-Damm and Z. Damm, in J. Keller and E. Robens (Eds.) 'Microbalance Techniques', Multi – Science Publishing, Brentwood 1994, p. 169.
8 G. W. Chądzyński, J. Stępień-Damm and Z. Damm, Pol. J. Chem., 68 (1994) 125.
9 M. Kelsey and R. Truttmann, International Laboratory, May 1997, p. 16.
10 J. Groszkowski, 'High Vacuum Techniques', WNT, Warsaw 1978.
11 J. Yarwood (Ed.) 'Vacuum and Thin Film Technology', Pergamon, Oxford 1978.
12 H. Kubicka and G. W. Chądzyński, Pol. J. Chem., 55 (1981) 1563.
13 H. Kubicka and G. W. Chądzyński, Heterogeneous Catalysis, Proc. 4th Int. Symp. on Heterogeneous Catalysis, Varna, Oct. 5–8, 1979, Bulg. Akad. Nauk, Sofia 1979, Vol 2, p. 457.
14 H. C. Yao and M. Shelef, J. Catal., 44 (1976) 392.
15 M. A. Ryashentseva and Kh. M. Minachev, Renij i Jego Sojedinenija w Geterogennom Katalize, Nauka, Moscow 1983.
16 G. W. Chądzyński and H. Kubicka, Thermochim. Acta, 158 (1990) 369.
17 M. J. D. Low, Chem. Rev., 60 (1960) 267.
18 C. Aharoni and F. C. Tompkins, Adv. Catal., 21 (1970) 1.
19 C. Aharoni, Adsorpt. Sci. Technol., 1 (1984) 1.
20 A. Cimino, B. A. De Angelis, D. Gazzoli and M. Valigi, Z. Anorg. Allg. Chem., 460 (1980) 86.